Journal of the European Ceramic Society 17 (1997) 71–76

PII: S0955-2219(96)00072-6
0955-2219/97/$17.00

Corrosion Screening Tests of High-Performance Ceramics in Supercritical Water Containing Oxygen and Hydrochloric Acid

Nikolaos Boukis,[a] Nils Claussen,[b] Klaus Ebert,[a] Rolf Janssen[b] & Michael Schacht[a]

[a]Institute for Technical Chemistry, Research Center Karlsruhe, Germany
[b]Advanced Ceramics Group, TU Hamburg–Harburg, Germany

(Received 12 February 1996; revised version received 1 March 1996; accepted 28 March 1996)

Abstract

The corrosion of various ceramic materials in simulated supercritical water oxidation (SCWO) environment was measured. Supercritical water with 0·44 mol kg^{-1} oxygen and 0·05 mol kg^{-1} hydrochloric acid was used to simulate typical SCWO conditions after the decomposition of the organic material. The experimental temperature was 465°C and the pressure 25 MPa. The experiments were performed within a reactor with an inner surface made of alumina. In this very corrosive fluid only a few Al_2O_3- and ZrO_2-based materials did not corrode severely. Homogeneous surface attack and grain boundary diffusion were observed. HIP-BN, B_4C, TiB_2, Y_2O_3 and Y-TZP disintegrated. SiC- and Si_3N_4-based materials showed a large weight loss, up to above 90%. © 1996 Elsevier Science Limited.

1 Introduction

The oxidation of organic hazardous wastes with oxygen or air in supercritical water (600°C > T > 374°C, 35 MPa > p > 22 MPa) is a promising new technology[1,2] often called the SCWO process. Under these conditions oxygen and most of the organics become soluble in water. In this single fluid phase organics are rapidly and quantitatively oxidized to CO_2, N_2 and H_2O. Species like Cl, S or P are converted to the acids HCl, H_2SO_4 and H_3PO_4, respectively. In 1994 the first commercial installation started operation with the destruction of amines, glycols and long-chain alcohols in Texas,[3] while several other units are under construction.[4,5] Further applications in the USA are the destruction of rocket fuels and explosives, warfare agents and organics in low radioactive liquid wastes.[6] In Germany and Japan, experimental work is focused on the destruction of industrial aqueous toxic wastes.[2,7]

The combination of high temperatures, high fluid density, oxygen and corrosive inorganic species leads to fast corrosion of almost all metallic alloys used for aggressive chemical environments. Engineers try to avoid corrosion by improved reactor design like 'transpiring walls'.[8] Another approach is the construction of reactors where the inner surface at the positions with the worst corrosion[9] is made of ceramic materials or coatings.[10] However, almost no experimental results are available on the corrosion of ceramic materials in SCWO environments. Recently Hazlebeck *et al.*[11] reported that, 'all nickel alloys and ceramics were rapidly corroded ... in nearly all of the environments' without detailed numerical data. These experiments were performed at a pressure of 27·6 MPa and temperatures of 350, 450 and 550°C.

Garcia and Mizia[12] investigated the corrosion behaviour of plasma-sprayed multilayered ceramic rings with an Inconel 625 or titanium substrate. The top coats were titania, zirconia partially stabilized with 7% yttria or zirconia partially stabilized with 24% magnesia. Experimental conditions were 1800–8000 ppm Cl^-, as HCl, $CeCl_3$, $ZnCl_2$ and $PbCl_2$, pressures of 24 MPa and temperatures of 300–650°C. Under these conditions all the tested coatings, except a titania multilayered ceramic system sprayed onto a titanium ring, failed because of blistering, cracking, peeling, erosion or delamination.

2 Experimental Procedures

An apparatus with a highly resistant reactor has been constructed for these experiments. The tube

reactor used is made of Al_2O_3 (Degussit Al 23, Friatec AG) and has a length of 700 mm and an inner diameter of 5 mm. This tube is placed inside a high-pressure-resistant tube made of Inconel 625 with an outer diameter of 14·3 mm and an inner diameter of 8 mm. The middle part of the tube (0·4 m) is electrically heated to a temperature of about 465°C (measured inside the tube). Both ends of the tube are cooled to room temperature with water-cooled metal blocks. The heating and the cooling systems are fixed on the Inconel 625 tube.

The experimental pressure, about 25 MPa, is built up with high-pressure pumps (Bischoff). It is measured with sensors (Burster) and regulated with an electropneumatic pressure regulator (TESCOM).

The periphery of the apparatus consists mainly of Ti or PEEK 1/16" tubing. Fittings from Autoclave Engineers are used for connection between the periphery of the apparatus and the reactor.

To avoid an extra compressor for oxygen or air, hydrogen peroxide is used as oxidant. The hydrogen peroxide is decomposed to water and oxygen — due to the high temperature — in the first part of the tube, far ahead of the position of the specimens. The aqueous solution used for the corrosion experiments contained 3% H_2O_2 and 0·05 mol kg^{-1} HCl (corresponding to 0·44 mol kg^{-1} O_2 and about 1800 ppm Cl^-). Under the typical experimental conditions (T = 465°C and P = 25 MPa) the density of the solution is 0·1 kg l^{-1}.[13]

In this screening test, the corrosion resistance of several commercial ceramic materials together with some ceramic composites developed by the Advanced Ceramics Group (ACG) of TUHH was qualitatively characterized by microscopy, weight loss and thickness of the corroded layer. These materials were cut to form small (e.g. 10 × 3 × 3 mm^3) specimens. The surface of the specimens before exposure was smooth but not polished. The corrosion experiments lasted 80–220 h.

To shorten the time required for these screening tests, each run was usually performed with five samples simultaneously. Most of the experiments were interrupted and started again due to numerous technical problems; some of these problems related to disintegration of the specimens.

For optical observations, a microscope with 350 fold magnification (Leica) and a CCD camera (JVC) with a digitizing system screen machine from Fast Electronics were used. For the surface analysis of corroded specimens, X-ray fluorescence elementary analysis (XRF; Siemens SRS 303) and a scanning electron microscope (SEM; Camscan FE 44) together with an energy-dispersive X-ray (EDX) system (Noran) were used.

3 Results

A compilation of all corrosion results is given in Table 1 together with the composition of the samples. Details of the materials are given in the respective references. The commercial materials are designated with the company codes.

3.1 Al_2O_3 base materials

The monolithic Al_2O_3 samples S1, S2 and S3 were exposed for 144, 220 and 140 h respectively, and no weight change was detected after the experiment. Merely, the original light beige colour of S2 was changed to a lighter tone after the exposure. This could not be assigned to any measurable specific change of the ceramic. However, the corrosion resistance of Al_2O_3 under these experimental conditions is better than the corrosion data reported elsewhere (up to 52 mg cm^{-2} in 168 h) which were obtained in more concentrated HCl solutions at temperatures lower than 245°C and at ambient pressure.[21–24]

Among the mixed alumina and zirconia ceramics, S4 showed excellent corrosion resistance under the experimental conditions. For sample S5, the exposure in the corrosive fluid caused a thick corroded layer (up to 1350 μm). Large cracks became visible (Fig. 1) and the corrosion was accelerated in regions near the cracks because the corrosive fluid could penetrate into the bulk of the material.

Specimens S6 and S7 altered their surface colour from light grey to white after exposure. The layer with changed colour extended up to 230–260 μm and 310 μm, respectively. EDX measurements revealed no major changes in the chemical composition in this layer. A scanning electron micrograph of the cross-section (S7, see Fig. 2) shows the intact body of the ceramic and pores (diameter < 1 μm) in the attacked outer layer. Therefore, the mechanical properties of ZrO_2-toughened alumina are expected to be reduced. The addition of non-oxide hard particles (20 vol% TiC/TiN, S8), on the other hand, also reduced the corrosion resistance. The specimen lost weight, its surface became rough and several holes with a diameter of 10–100 μm were observed. However, the corroded layer was very thin, indicating homogeneous surface attack rather than grain boundary corrosion.

3.2 Mullite matrix composites

Two different mullite matrix composites (reaction formed) were tested: (1) fabricated via oxidation of Al and subsequent reaction of alumina and zircon (S9 and S10) and (2) based on the oxidation of Al and SiC and subsequent mullitization (S11–S13), the latter containing a certain amount of SiC

Table 1. Corrosion behaviour of several ceramic materials tested in supercritical water

Code	*Composition (wt%)*	*Exposure time (h)*	*dG/A (mg cm^{-2})*	*Corroded layer (μm)*	*Remarks*	*Ref.*
S1	Sapphire	144	<0·1	<10	Saphicon USA	
S2	99·7% Al_2O_3	220	<0·1	<10	Friatec Degussit A123	
S3	99·7% Al_2O_3	140	<0·1	<10	Vesuvius Zyalox 99·7	
S4	90% Al_2O_3, 10% ZrO_2	150	<0·1	<10	Krupp Widia WDX-U	
S5	90% Al_2O_3, 10% ZrO_2	143	0·33	1150–1350	Cerasiv DN 70	
S6	80% Al_2O_3, 18% ZrO_2	143	0·79	230–260	ACG, reaction-bonded alumina	14
S7	Al_2O_3, ZrO_2 (3% Y_2O_3)	133	0·31	310	ACG, sintered in air at 1500°C	
S8	72% Al_2O_3, 8% ZrO_2, 20% TiC/TiN	150	5·25	<10	Krupp Widia WDX-H	
S9	60% mullite, 40% ZrO_2	144	0·27	<10	ACG, reaction-bonded mullite (RBM)	15
S10	60% mullite, 10% Al_2O_3, 30% ZrO_2	133	1·76	500–600	ACG, RBM	15
S11	70% mullite, 10% SiC, 15% ZrO_2, 5% Al_2O_3	144	2·28	170–220	ACG, RBM matrix composite	16
S12	70% mullite, 10% SiC, 15% ZrO_2, 5% Al_2O_3	143	1·74	35–60	ACG, sample 11, postHIPed	16
S13	50% mullite, 40% SiC, 10% ZrO_2	133	13·09	350–500	ACG, RBM matrix composite	16
S14	97 mol% ZrO_2, 3 mol% Y_2O_3	9	disintegrated	–	ACG, 3Y-TZP	17
S15	96·5 mol% ZrO_2, 3·5 mol% Y_2O_3	2	disintegrated	–	Tosoh	
S16	89·5% ZrO_2, 10·5% Y_2O_3	140	disintegrated	–	Vesuvius Zyazirc, Z 105	
S17	96·5 mol% ZrO_2, 3·5 mol% MgO	220	<0·1	<10	Friatec FZM	
S18	92·1 mol% ZrO_2; 7·1 mol% MgO; 0·8 mol% Y_2O_3 + 3 vol% spinel	144	0·36	<10	ACG, Mg,Y-PSZ	18
S19	91·7 mol%ZrO_2, 7·8 mol% MgO, 0·5 mol% Y_2O_3 + 3 vol% spinel	140	+ 0·76[a]	<10	ACG, Mg, Y-PSZ	19
S20	91·7 mol% ZrO_2, 7·8 mol% MgO, 0·5 mol% Y_2O_3 + 3 vol% spinel	140	+ 0·56[a]	<10	ACG, HIP-Mg, Y-PSZ	19
S21	> 99% Si_3N_4, free Si < 1%	144	129·49	<10	ACG, reaction-bonded silicon nitride (RBSN)	20
S22	93% Si_3N_4, 5% Y_2O_3, 2% Al_2O_3	150	51·93	<10	ACG, HIP-RBSN	20
S23	> 79% Si_3N_4, 20% SiC platelets, free Si < 1%	135	61·36	<10	ACG, SiC-platelet reinforced RBSN	20
S24	74% Si_3N_4, 19% SiC platelets, 5% Y_2O_3, 2% Al_2O_3	143	55·69	<10	ACG, SiC-platelet reinforced HIP-RBSN	20
S25	Si_3N_4–TiC/TiN	143	59·81	300	Krupp Widia N 2000	
S26	β-Sialon, $Si_{5.3}Al_{0.7}O_{0.7}N_{7.3}$	150	74·19	400	MPI[b]	
S27	S-SiC	133	ca. 75	–	Toshiba (bearing)	
S28	ca. 99% SiC, ca. 1% Al_2O_3	150	33·93	<10		
S29	AlN	80	+4·83[a]		Sintec	
S30	B_4C	80	disintegrated	–	Goodfellow	
S31	BN	80	disintegrated	–	Sintec	
S32	TiB_2	80	disintegrated	–	Sintec	
S33	Y_2O_3	80	disintegrated	–	Goodfellow	

[a]Weight gain.
[b]Max Planck Institute of Metals Research, Stuttgart, Germany.

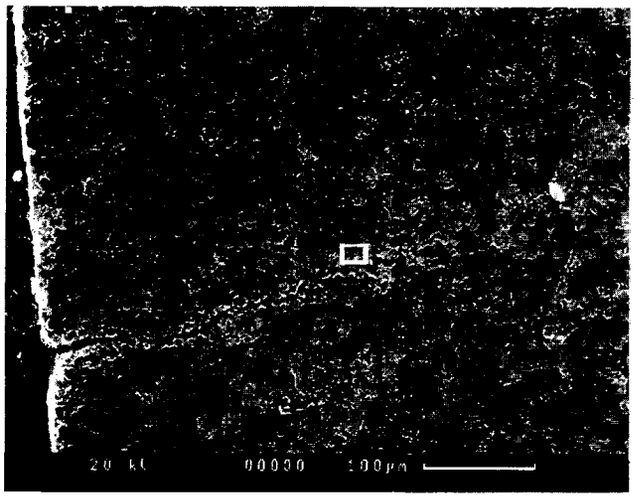

Fig. 1. Crack in the corroded layer of S5 (90% Al_2O_3 and 10% ZrO_2).

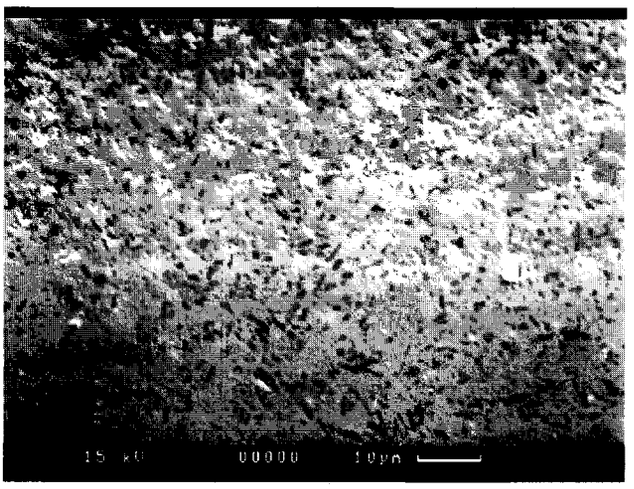

Fig. 2. Cross-section of S7 (Y_2O_3-stabilized ZrO_2-toughened Al_2O_3) with the corroded, porous outer layer.

particles that remained unreacted during synthesis. The zircon-based materials exhibit a low-to-moderate corrosion resistance, although the corroded layer of one batch (S10) partially peeled off during exposure. The SiC-based mullite materials showed lower corrosion resistance (S11 and S13), only the sample densified by post hot-isostatic press(HIP)ing exhibiting moderate damage resistance (S12). These three samples changed colour from grey to white, and the Si EDX signal in the corroded layer was considerably lower than that in the untreated sample indicating that SiC particles are removed preferentially during the corrosion test. Presumably the SiC particles are first oxidized and then dissolved in the supercritical steam according to the reaction $2SiO_2 + 3H_2O \rightarrow Si_2O(OH)_6$,[25,26] leading to enhanced porosity and the formation of an alumina layer (approximately 7 μm) on top of the corroded surface of the mullite composites (Fig. 3).

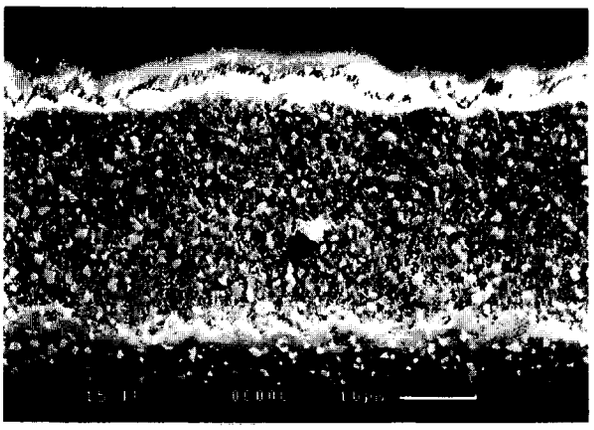

Fig. 3. Cross-section of S12 (HIP reaction-bonded mullite–SiC) with the top layer of Al_2O_3 and a thicker porous layer.

3.3 ZrO_2 base materials

Y-TZP materials (S14–S16) tended to disintegrate after some hours of exposure, presumably due to $t \rightarrow m$ phase transformation.[27–29] The PSZ materials, on the other hand, were more stable against disintegration. For these specimens (S17–S20) the weight loss was negligible. The surface of sample S20 showed many cracks (up to 250 μm deep) on the surface caused by lattice transformation from tetragonal to monoclinic.

The amount of m-ZrO_2 on the surface of corroded S20 was 37%. The HIP-Mg, Y-PSZ originally consisted of 7% monoclinic ZrO_2, 30% tetragonal ZrO_2 and 63% cubic ZrO_2*. This means that all tetragonal ZrO_2 on the surface was transformed to monoclinic ZrO_2 during the exposure (Fig. 4).

3.4 Si_3N_4 base materials

All the tested Si_3N_4 materials corroded severely under the experimental conditions mentioned above. Sample S21 originally had an open porosity of 20% due to the production process, which resulted in considerable dissolution during exposure due to the large surface area. Therefore, the HIPed sample S22 showed an enhanced corrosion resistance compared with S21. The Si_3N_4–TiC/TiN composite (S25) was covered with a white, brittle layer (300 μm thick). The weight loss was high, even before removing the brittle layer. Sialon S26 also developed a white, brittle, 400 μm thick layer during treatment, which consisted mainly of Al_2O_3. Silicon was selectively dissolved from this layer according to the XRF measurement. The addition of 20% SiC to Si_3N_4 (S23 and S24) did not enhance the corrosion resistance. The corrosion on these composites proceeded like that of the monolithic Si_3N_4 samples (S21 and S22) via surface attack, leading to a rather thin corrosion layer.

*X-ray diffraction measurement performed by F. Meschke, TUHH.

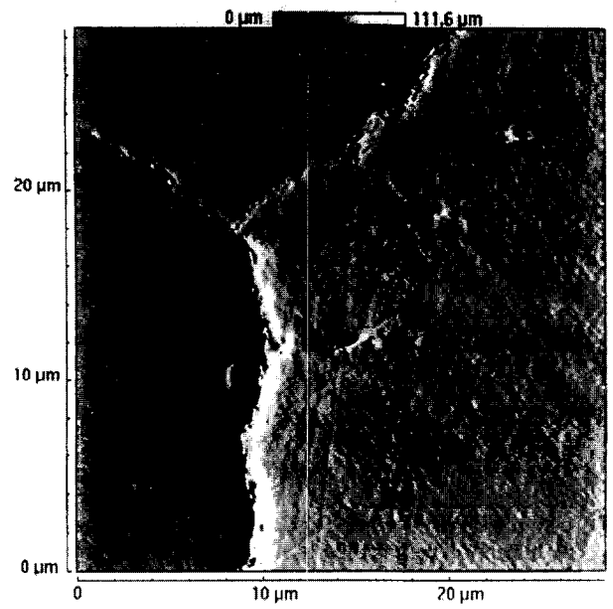

Fig. 4. Cross-section of S20 with cracks, due to the phase transformation from tetragonal ZrO_2 to monoclinic (atomic force microscopy test measurement by Surface Imaging Systems GmbH).

3.5 SiC base materials

Although silicon carbide is more resistant than silicon nitride under the given experimental conditions, sample S27 showed a white, brittle layer and a high weight loss. No surface layer was formed on S28 but the weight loss was similar to that of S27.

3.6 Various ceramic materials

The other ceramic materials tested (S29–S33) were not stable under the experimental conditions and most of them disintegrated. AlN (S29) was covered with a white, 300 μm thick layer and showed a weight gain due to the oxidation of AlN, forming Al_2O_3.

4 Conclusion

Most of the ceramic materials tested except monolithic alumina and PSZ showed a low corrosion resistance against HCl- and O_2-containing supercritical aqueous solution under the experimental conditions (T = 465°C, P = 25MPa, density = 0·1 kg l^{-1}). The corrosion proceeds predominantly either by homogeneous surface attack or by grain boundary diffusion, resulting in severe weight losses or disintegration after 1·5–140 h exposure. On the other hand, this screening test identified alumina and PSZ as candidate materials for bulk liners or protective coatings in the SCWO technology. Further experiments will be carried out in the near future to analyse the corrosion resistance of these materials in various acidic solutions at supercritical conditions.

Acknowledgment

We would like to thank Dr J. Römer and W. Habicht from the Research Center Karlsruhe for performing the SEM, EDX and XRF analyses. We would also like to thank colleagues from the TU Hamburg–Harburg, especially F. Meschke for producing some of the tested materials and the X-ray diffraction analysis.

References

1. Modell, M., Processing methods for the oxidation of organics in supercritical water. US Patent 4 338 199, 6 July 1982.
2. Ebert, K. H. & Franck, E. U., Potentials & Needs of SCWO in future technologies in Europe. In *Proc. First Int. Workshop on Supercritical Water Oxidation*, Amelia Island, FL, 6–9 February 1995. WCM Forums, Lake Bluff, IL.
3. McBrayer, R., Development and operation of the first supercritical wet oxidation industrial waste destruction facility. In *Proc. First Int. Workshop on Supercritical Water Oxidation*, Amelia Island, FL, 6–9 February 1995. WCM Forums, Lake Bluff, IL.
4. Welland, H. J., Hydrothermal oxidation of hazardous waste pilot plant test bed. In *Proc. First Int. Workshop on Supercritical Water Oxidation*, Amelia Island, FL, 6–9 February 1995. WCM Forums, Lake Bluff, IL.
5. Wiegand, G., Oxidation in supercritical water. In *Proc. First Int. Workshop on Supercritical Water Oxidation*, Amelia Island, FL, 6–9 February 1995. WCM Forums, Lake Bluff, IL.
6. Hart, P. W., Treatment of U.S. DOE mixed waste using SCWO technology. In *Proc. First Int. Workshop on Supercritical Water Oxidation*, Amelia Island, FL, 6–9 February 1995. WCM Forums, Lake Bluff, IL.
7. Suzuki, A., Construction of the first SCWO pilot-scale plant in Japan. In *Proc. First Int. Workshop on Supercritical Water Oxidation*, Amelia Island, FL, 6–9 February 1995. WCM Forums, Lake Bluff, IL.
8. Mueggenburg, H. H., Rousar, D. C. & Young, M. F., SCWO reactor with water conduits for boundary flow control. US Patent 5 387 398, 7 February 1995.
9. Boukis, N., Landvatter, R., Habicht, W., Franz, G., Leistikow, S., Kraft, R. & Jacobi, O., First experimental SCWO corrosion results of Ni-base alloys fabricated as pressure tubes and exposed to oxygen containing diluted hydrochloric acid at $T \leq 450$°C, P = 24 MPa. In *Proc. First Int. Workshop on Supercritical Water Oxidation*, Amelia Island, FL, 6–9 February 1995. WCM Forums, Lake Bluff, IL.
10. Hong, G., Killilea, W. & Ordway, D., Zirconium oxide ceramics for surfaces exposed to high temperature water oxidation environments. PCT Int. Appl. No 92/18428, 1992, 45 pp.
11. Hazlebeck, D. A., Downey, K. W., Elliott, J. P. & Spritzer, M. H., Design of corrosion resistant HTO systems for DoD hazardous wastes. In *Proc. First Int. Workshop on Supercritical Water Oxidation*, Amelia Island, FL, 6–9 February 1995. WCM Forums, Lake Bluff, IL.
12. Garcia, K. M. & Mizia, R., Corrosion investigation of multilayered ceramics and experimental nickel alloys in SCWO process environments. In *Proc. First Int. Workshop*

on Supercritical Water Oxidation, Amelia Island, FL, 6–9 February 1995. WCM Forums, Lake Bluff, IL. And also under the same title: INEL-94/0017, Lockheed Idaho Technologies Company, Idaho Falls, ID, February 1995.
13. Haar, L., Gallagher, J. S. & Kell, G. S., *NBS/NRC Steam Tables*. Hemisphere Publishing Corporation, Washington — New York — London.
14. Holz, D., Wu, S., Scheppokat, S. & Claussen, N., Effect of processing parameters on phase and microstructure evolution in RBAO-ceramics. *J. Am. Ceram. Soc.*, **77** (1994) 2509–2517.
15. Lathabai, S., Hay, D. G., Wagner, F. & Claussen, N., Reaction bonded mullite zirconia composites. *J. Am. Ceram. Soc.*, **79** (1996) 248–256.
16. Wu, S. & Claussen, N., Reaction bonding and mechanical properties of mullite/SiC composites. *J. Am. Ceram. Soc.*, **77** (1994) 2898–2904.
17. Knechtel, M. C., Garcia, D. E., Rödel, J. & Claussen, N., Subcritical crack growth in Y-TZP and Al_2O_3-toughened Y-TZP. *J. Am. Ceram. Soc.*, **76** (1993) 2681–2684.
18. Meschke, F., de Portu, G. & Claussen, N., Microstructure and thermal stability of finegrained (Y, Mg)-PSZ ceramics with alumina additions. *J. Eur. Ceram. Soc.*, **11** (1993) 481–486.
19. Meschke, F., Claussen, N., de Portu, G. & Rödel, J., Interrelation between strength, flaw size, transformability and R-curve behavior in fine-grained Mg, Y-PSZ. *Fourth Euro-Ceramics*, **3** (1995) 161–168.
20. Janssen, R. & Claussen, N., SiC-platelet reinforcement of Si_3N_4 composites. In *Proc. Int. Symp. on Science of Engineering Ceramics*, eds S. Kimura & K. Niihara. Ceramic Society of Japan, Tokyo, 1991 pp. 371–378.
21. Dawihl, W. & Klingler, E., Der Korrosionswiderstand von Aluminiumoxideinkristallen und von gesinterten Werkstoffen auf Aluminiumoxidgrundlage gegen anorganische Säuren. *Ber. DKG*, **44** (1967) 1–4.
22. Genthe, W. & Hausner, H., Corrosion of alumina in acids. In *Euroceramics*, eds G. de Wirth & R. A. Terpstra. Elsevier Applied Science, London, 1989, pp. 3463–3467.
23. Genthe, W. & Hausner, H., Influence of chemical composition on corrosion of alumina in acids and caustic solutions. *J. Eur. Ceram. Soc.*, **9** (1992) 417–425.
24. Genthe, W. & Hausner, H., Korrosionsverhalten von Aluminiumoxid in Säuren und Laugen. *cfi/Ber. DKG*, **67** (1990) 6–11.
25. Franck, E. U., Report on Dechema colloquium. *Werkstoffe u Korrosion*, **11** (1969) 140.
26. Brady, E. L., *J. Phys. Chem.*, **57** (1963) 706–710, cited in *Corrosion Handbook*, Vol. 1, VCH, Weinheim, Germany.
27. Yoshimura, M., Noma, T., Kawabata, K. & Somiya, S., The effects of high temperature and high pressure water on the low temperature degradation behavior of Y-TZP. *J. Ceram. Soc. Jpn Int. Edn*, **96** (1988) 263–268.
28. Nakajima, K., Kobayashi, K. & Murata, Y., Phase stability of Y-TZP in aqueous solutions. In *Advances in Ceramics*, Vol. 12, eds N. Claussen, M. Rühle & A. Heuer. The American Ceramic Society, Columbus, OH, 1983 pp. 399–407.
29. Sato, T. & Shimada, M., Transformation of yttria-doped ZrO_2 polycrystals by annealing in water. *J. Am. Ceram. Soc.*, **68** (1985) 356–359.